

Combination of Lacunary Polyoxometalates and High-Nuclear Transition Metal Clusters under Hydrothermal Conditions.

3. Structure and Characterization of

$[\text{Cu}(\text{enMe})_2]_2\{[\text{Cu}(\text{enMe})_2(\text{H}_2\text{O})]_2[\text{Cu}_6(\text{enMe})_2(\text{B}-a\text{-SiW}_9\text{O}_{34})_2]\}\cdot 4\text{H}_2\text{O}$

Shou-Tian Zheng,[†] Da-Qiang Yuan,[†] Jie Zhang,[†] and Guo-Yu Yang^{*,†,‡}

State Key Laboratory of Structural Chemistry, Fujian Institute of Research on the Structure of Matter, Chinese Academy of Sciences, Fuzhou, Fujian 350002, China, and State Key Laboratory of Coordination Chemistry, Nanjing University, Nanjing, Jiangsu 210093, China

Received January 30, 2007

A novel sandwich-type polyoxometalate incorporating a unique hybrid hexanuclear copper cluster, $[\text{Cu}(\text{enMe})_2]_2\{[\text{Cu}(\text{enMe})_2(\text{H}_2\text{O})]_2[\text{Cu}_6(\text{enMe})_2(\text{B}-a\text{-SiW}_9\text{O}_{34})_2]\}\cdot 4\text{H}_2\text{O}$ (**1**, enMe = 1,2-diaminopropane), has been hydrothermally synthesized and structurally characterized by the elemental analyses, IR spectroscopy, TG analysis, magnetic properties, and single-crystal X-ray diffraction analysis. Crystal data for **1**: triclinic, $P\bar{1}$; $a = 12.5105(2)$, $b = 14.3710(2)$, $c = 17.2687(2)$ Å; $\alpha = 98.834(1)$, $\beta = 110.744(1)$, $\gamma = 104.711(1)^\circ$; $V = 2704.57(7)$ Å³; $\rho = 3.646$ g/cm³; $Z = 1$. X-ray crystallographic study shows that the molecular structure of **1** contains 10 copper ions: Six of them form an unprecedented inorganic–organic hybrid Cu_6 cluster via edge-sharing combination of two CuO_6 octahedra, two CuO_5 , and two CuO_3N_2 square pyramids and are encapsulated between two $\{\text{B}-a\text{-SiW}_9\text{O}_{34}\}$ units. Two of them form two $[\text{Cu}(\text{enMe})_2(\text{H}_2\text{O})]^{2+}$ complexes and further attach to the two $\{\text{B}-a\text{-SiW}_9\text{O}_{34}\}$ units via two $\text{Cu}-\text{O}=\text{W}$ bridges, acting as a decorated role. The remaining two form isolated $[\text{Cu}(\text{enMe})_2]^{2+}$ complexes playing roles of charge-compensation and space-fillers. Magnetization measurement reveals that the hexanuclear copper cluster exhibits overall ferromagnetic interactions.

Introduction

Transition-metal-substituted polyoxometalates (TMSPs) based on lacunary precursors derived from Keggin and Dawson polyanions exhibit a fascinating variety of structures and properties including catalysis, medicine, and magnetism.^{1–2} The lacunary anions, such as monovacant ($\alpha\text{-PW}_{11}\text{O}_{39}$, $\alpha\text{-P}_2\text{W}_{17}\text{O}_{61}$), divacant ($\gamma\text{-SiW}_{10}\text{O}_{36}$), and trivacant ($\alpha\text{-PW}_9\text{O}_{34}$, $\alpha\text{-P}_2\text{W}_{15}\text{O}_{56}$), were proved to have well-defined metal–cation binding sites and can incorporate a variety of TMs or rare earths including Mn, Fe, Co, Ni, Cu, Zn, Zr,

Pd, La, Ce, Y, Nd, Gd, and so on. The incorporated metal cations provide sufficiently strong linkages to connect the lacunary anions into stable and large clusters. To date, TMSPs containing from 1 to 12 lacunary precursors and from 1 to 28 TMs have been obtained.^{3–4} Since materials properties are intricately linked to their structural features, the creation of novel TMSP structural types is still attractive in modern chemistry though a vast amount of work has been reported.

So far, though hydrothermal techniques have been widely applied to making polyoxometalates (POMs),⁵ most of reported TMSPs were prepared by conventional solution syntheses at atmospheric pressure and relatively low temperature (below 100 °C).^{3,4,6–10} Currently, we are exploring the applicability of trilacunary Keggin XW_9O_{34} fragments and paramagnetic TM ions for the synthesis of new magnetically attractive TMSPs under hydrothermal conditions. Our strategy is based on the following considerations: (1) The trilacunary sites of XW_9O_{34} unit may act as the structure-directing agent that induces the paramagnetic TM ions to

* To whom correspondence should be addressed. E-mail: ygy@fjirm.ac.cn. Fax: +86-591-83710051.

[†] Chinese Academy of Sciences.

[‡] Nanjing University.

(1) (a) *Polyoxometalate Chemistry: From Topology via Self-Assembly to Applications*; Pope, M. T., Müller, A., Eds.; Kluwer: Dordrecht, The Netherlands, 2001. (b) *Polyoxometalate Molecular Science*; Borrás-Almenar, J. J., Coronado, E., Müller, A., Pope, M. T., Eds.; Kluwer: Dordrecht, The Netherlands, 2004.

(2) (a) *Polyoxometalates*; Hill, C. L., Ed.; *Chem. Rev.* **1998**. (b) Pope, M. T. *Comput. Coord. Chem.* **2003**, *4*, 635. (c) Hill, C. L. *Comput. Coord. Chem.* **2003**, *4*, 679.

undergo large TM cluster aggregations under the rational hydrothermal conditions and differs from the invisible structure-directing agent of lone pair electron in Se^{IV} .¹¹ (2) The lacunary XW_9O_{34} and the paramagnetic TM cluster aggregations formed in-situ may be used as structural building units and subtly combined to produce novel discrete or extended high-nuclear TMSPs.

Following this strategy, we report here the hydrothermal synthesis and structure of a novel Cu_6 -containing sandwich TMSPs: $[\text{Cu}(\text{enMe})_2]_2\{[\text{Cu}(\text{enMe})_2(\text{H}_2\text{O})]_2[\text{Cu}_6(\text{enMe})_2(B-a\text{-SiW}_9\text{O}_{34})_2]\} \cdot 4\text{H}_2\text{O}$ **1** (enMe = 1,2-diaminopropane). To date, numerous sandwich TMSPs based on two $[\text{XW}_9\text{O}_{34}]^{n-}$ ($\text{X} = \text{Si}, \text{P}, \text{As}$) or $[\text{X}_2\text{W}_{15}\text{O}_{56}]^{12-}$ ($\text{X} = \text{P}, \text{As}$) fragments and three or four TM centers have constituted a well-known class of POMs.³ At present, it is a great challenge and structural interest to make sandwich TMSPs incorporating more than four TMs. Up to now, only several sandwich TMSPs incorporating more than four TMs have been reported,^{6–10} such as $[\text{Fe}_6(\text{OH})_3(A-\alpha\text{-GeW}_9\text{O}_{34}(\text{OH})_3)_2]^{11-}$,⁶ $[\text{Ni}_6(\text{H}_2\text{O})_4(\mu_2\text{-H}_2\text{O})_4(\mu_3\text{-OH})_2](\chi\text{-SiW}_9\text{O}_{34})_2]^{10-}$, and $[\text{Ni}_7(\text{OH})_4(\text{H}_2\text{O})(\text{CO}_3)_2(\text{HCO}_3)(A-\alpha\text{-SiW}_9\text{O}_{34})(\beta\text{-SiW}_{10}\text{O}_{37})]^{10-}$.⁷ For the family of Cu-containing sandwich TMSPs, Kortz and Yamase recently reported the synthesis and magnetism of the first Cu_5 -/ Cu_6 -containing sandwich polyoxoanions $[\text{Cu}_5(\text{OH})_4(\text{H}_2\text{O})_2(A-a\text{-SiW}_9\text{O}_{33})_2]^{10-}$ ⁸ and $[(\text{CuCl})_6(\text{AsW}_9\text{O}_{33})_2]^{12-}$,⁹ respectively. Now, **1** exhibits the second sandwich POM incorporating Cu_6 cluster but the first Cu_6 -containing tungstosilicate. Furthermore, the structure of the Cu_6 cluster in **1** has never been observed, either in the rich domain of POMs or in coordination chemistry.

Experimental Section

All chemicals employed in this study were analytical reagent and purchased from commercial sources. Elemental analyses of C, H, and N were carried out with a Vario EL III elemental analyzer. IR spectra (KBr pellets) were recorded on an ABB Bomen MB 102 spectrometer. Thermal analysis was performed in a dynamic oxygen atmosphere with a heating rate of 10 °C/min, using a Mettler TGA/SDTA851^e thermal analyzer. Variable-temperature susceptibility measurements were carried out in the temperature range 2–300 K at a magnetic field of 1 T on polycrystalline samples with a Quantum Design PPMS-9T magnetometer. The experimental susceptibilities were corrected for Pascal's constants.

Synthesis of 1. A mixture of $\text{Na}_9[A-\alpha\text{-SiW}_9\text{O}_{34}] \cdot n\text{H}_2\text{O}$ (0.80 g, prepared by literature method),¹² $\text{CuCl}_2 \cdot 2\text{H}_2\text{O}$ (0.17 g), enMe (0.10 mL), and H_2O (10 mL) was stirred for 40 min. The mixture was then transferred to a Teflon-lined stainless steel autoclave (40 mL) and kept at 160 °C for 3 days and then cooled to room temperature. The solid product, consisting of single crystals in the form of blue blocks, was recovered by filtration, washed with distilled water, and dried in air (19.2% yield based on Cu). It is notable that **1** was not obtained by solution synthesis at atmospheric pressure. Elemental analysis showed that the sample contains 5.96, 2.03, and 4.61 wt % of C, H, and N, respectively, in well accord with the expected values of 6.06, 1.90, and 4.72 wt % of C, H, and N on the basis of the empirical formula given by the single-crystal structure analysis. IR (KBr, cm^{-1}) for **1**: 3439 (s), 2962 (w), 1632 (s), 1582 (s), 1448 (w), 1381 (w), 1348 (w), 1063 (m), 946 (s), 888 (s), 771 (s), 737 (s), 511 (m).

X-ray Analysis. Suitable single crystal with dimensions of 0.25 × 0.22 × 0.15 mm was selected for single-crystal X-ray diffraction

- (3) (a) Weakley, T. J. R.; Evans, H. T.; Showell, J. S.; Tourné, G. F.; Tourné, C. M. *J. Chem. Soc., Chem. Commun.* **1973**, 139. (b) Finke, R. G.; Droegge, M.; Hutchinson, J. R.; Gansow, O. *J. Am. Chem. Soc.* **1981**, *103*, 1587. (c) Wasfi, S. H.; Rheingold, A. L.; Kokozka, G. F.; Goldstein, A. S. *Inorg. Chem.* **1987**, *26*, 2934. (d) Weakley, T. J. R.; Finke, R. G. *Inorg. Chem.* **1990**, *29*, 1235. (e) Gómez-García, C. J.; Coronado, E.; Gómez-Romero, P.; Casañ-Pastor, N. *Inorg. Chem.* **1993**, *32*, 3378. (f) Gómez-García, C. J.; Borrás-Almenar, J. J.; Coronado, E.; Ouahab, L. *Inorg. Chem.* **1994**, *33*, 4016. (g) Zhang, X.; Jameson, G. B.; O'Connor, C. J.; Pope, M. T. *Polyhedron* **1996**, *15*, 917. (h) Zhang, X.; Chen, Q.; Duncan, D. C.; Campaña, C.; Hill, C. L. *Inorg. Chem.* **1997**, *36*, 4208. (i) Zhang, X.; Chen, Q.; Duncan, D. C.; Lachicotte, R. J.; Hill, C. L. *Inorg. Chem.* **1997**, *36*, 4381. (j) Clemente-Juan, J. M.; Coronado, E.; Galán-Mascarós, J. R.; Gómez-García, C. J. *Inorg. Chem.* **1999**, *38*, 55. (k) Bi, L.; Wang, E.; Peng, J.; Huang, R.; Xu, L.; Hu, C. *Inorg. Chem.* **2000**, *39*, 671. (l) Bi, L.; Huang, R.; Peng, J.; Wang, E.; Wang, Y.; Hu, C. *J. Chem. Soc., Dalton Trans.* **2001**, 121. (m) Kortz, U.; Al-Kassem, N. K.; Savelieff, M. G.; Kadi, N. A. A.; Sadakane, M. *Inorg. Chem.* **2001**, *40*, 4742. (n) Anderson, T. M.; Hardcastle, K. I.; Okun, N.; Hill, C. L. *Inorg. Chem.* **2001**, *40*, 6418. (o) Kortz, U.; Mbomekalle, I. M.; Keita, B.; Nadjó, L.; Berthet, P. *Inorg. Chem.* **2002**, *41*, 6412. (p) Bi, L.; Kortz, U.; Keita, B.; Nadjó, L.; Borrmann, H. *Inorg. Chem.* **2004**, *43*, 8367. (r) Fang, X.; Anderson, T. M.; Benelli, C.; Hill, C. L. *Chem.—Eur. J.* **2005**, *11*, 712. (s) Kortz, U.; Nellutla, S.; Stowe, A. C.; Dalal, N. S.; Tol, J. V.; Bassil, B. S. *Inorg. Chem.* **2004**, *43*, 144.
- (4) (a) Mialane, P.; Dolbecq, A.; Marrot, J.; Rivière, E.; Sécheresse, F. *Angew. Chem., Int. Ed.* **2003**, *42*, 3523. (b) Godin, B.; Chen, Y. G.; Vaissermann, J.; Ruhlmann, L.; Verdaguer, M.; Gouzerh, P. *Angew. Chem., Int. Ed.* **2005**, *44*, 3072. (c) Hussain, F.; Bassil, B. S.; Bi, L. H.; Reicke, M.; Kortz, U. *Angew. Chem., Int. Ed.* **2004**, *43*, 3485. (d) Sadakane, M.; Dickman, M. H.; Pope, M. T. *Angew. Chem., Int. Ed.* **2000**, *39*, 2914. (e) Kim, G. S.; Zeng, H. D.; VanDerveer, D.; Hill, C. L. *Angew. Chem., Int. Ed.* **1999**, *38*, 3205. (f) Kortz, U.; Savelieff, M. S.; Bassil, B. S.; Dickman, M. H. *Angew. Chem., Int. Ed.* **2001**, *40*, 3384. (g) Wassermann, K.; Dickman, M. H.; Pope, M. T. *Angew. Chem., Int. Ed.* **1997**, *36*, 1445. (h) Mialane, P.; Dolbecq, A.; Marrot, J.; Rivière, E.; Sécheresse, F. *Chem.—Eur. J.* **2005**, *11*, 1771. (i) Fukaya, K.; Yamase, T. *Angew. Chem., Int. Ed.* **2003**, *42*, 654. (j) Howell, R. C.; Perez, F. G.; Jain, S.; Horrocks, W. D.; Rheingold, J. A. L.; Francesconi, L. C. *Angew. Chem., Int. Ed.* **2001**, *40*, 4031. (k) Kortz, U.; Hussain, F.; Reicke, M. *Angew. Chem., Int. Ed.* **2005**, *44*, 3773. (l) Mbomekalle, I. M.; Keita, B.; Nierlich, M.; Kortz, U.; Berthet, P.; Nadjó, L. *Inorg. Chem.* **2003**, *42*, 5143. (m) Kortz, U.; Jeannin, Y. P.; Tézé, A.; Hervé, G.; Isber, S. *Inorg. Chem.* **1999**, *38*, 3670. (n) Kortz, U.; Tézé, A.; Hervé, G. *Inorg. Chem.* **1999**, *38*, 2038. (o) Mialane, P.; Marrot, J.; Mallard, A.; Hervé, G. *Inorg. Chim. Acta* **2002**, *328*, 81.
- (5) (a) Khan, M. I.; Tabussum, S.; Doedens, R. J.; Golub, V. O.; O'Connor, C. J. *Inorg. Chem.* **2004**, *43*, 5850. (b) Tripathi, A.; Hughbanks, T.; Clearfield, A. *J. Am. Chem. Soc.* **2003**, *125*, 10528. (c) Whitfield, T.; Wang, X.; Jacobson, A. J. *Inorg. Chem.* **2003**, *42*, 3728. (d) Hargman, P. J.; Hargman, D.; Zubieta, J. *Angew. Chem., Int. Ed.* **1999**, *38*, 2638. (e) Burkholder, E.; Golub, V.; O'Connor, C. J.; Zubieta, J. *Inorg. Chem.* **2003**, *42*, 6729. (f) Pitzschke, D.; Wang, J.; Hoffmann, R. D.; Pöttgen, R.; Bensch, W. *Angew. Chem., Int. Ed.* **2006**, *45*, 1305. (g) Khan, M. I.; Yohannes, E.; Doedens, R. J. *Inorg. Chem.* **2003**, *42*, 3125. (h) Lin, B. Z.; Liu, S. X. *Chem. Commun.* **2002**, 2126.
- (6) Bi, L.; Kortz, U.; Nellutla, S.; Stowe, A. C.; Tol, J. V.; Dalal, N. S.; Keita, B.; Nadjó, L. *Inorg. Chem.* **2005**, *44*, 896.
- (7) Zhang, Z.; Li, Y.; Wang, E.; Wang, X.; Qin, C.; An, H. *Inorg. Chem.* **2006**, *45*, 4313.
- (8) (a) Bi, L.; Kortz, U. *Inorg. Chem.* **2004**, *43*, 7961. (b) Nellutla, S.; Tol, J. V.; Dalal, N. S.; Bi, L.; Kortz, U.; Keita, B.; Nadjó, L.; Khitrov, G. A.; Marshall, A. G. *Inorg. Chem.* **2005**, *44*, 9795.
- (9) Yamase, T.; Fukaya, K.; Nijiri, H.; Ohshima, Y. *Inorg. Chem.* **2006**, *45*, 7698.
- (10) Anderson, T. M.; Neiwert, W. A.; Hardcastle, K. I.; Hill, C. L. *Inorg. Chem.* **2004**, *43*, 7353.

(11) Rao, C. N. R.; Behera J. N.; Dan, M. *Chem. Soc. Rev.* **2006**, *35*, 375 and references therein.

(12) Tézé, A.; Hervé, G. *Inorganic Syntheses*; John Wiley & Sons: New York, 1990; Vol. 27, p 87.

Table 1. Crystallographic Data for **1**

empirical formula	C ₃₀ H ₁₁₂ Cu ₁₀ N ₂₀ O ₇₄ Si ₂ W ₁₈
Fw	5938.20
cryst system	triclinic
space group	<i>P</i> 1
<i>a</i> /Å	12.5105(2)
<i>b</i> /Å	14.3710(2)
<i>c</i> /Å	17.2687(2)
α /deg	98.8340(10)
β /deg	110.7440(10)
γ /deg	104.7110(10)
<i>V</i> /Å ³	2704.57(7)
<i>Z</i>	1
<i>D_c</i> /g cm ⁻³	3.646
μ /mm ⁻¹	21.091
<i>F</i> (000)	2673
θ range (deg)	2.16 $\leq \theta \leq$ 25.70
limiting indices	-13 $\leq h \leq$ 15, -17 $\leq k \leq$ 17, -21 $\leq l \leq$ 18
goodness-of-fit on <i>F</i> ²	1.070
<i>R</i> ₁ , ^a <i>wR</i> ₂ ^b [<i>I</i> > 2 σ (<i>I</i>)]	0.0471, 0.1122
<i>R</i> ₁ , ^a <i>wR</i> ₂ ^b (all data)	0.0607, 0.1239

^a *R*₁ = $\sum||F_o| - |F_c||/\sum|F_o|$. ^b *wR*₂ = $\{\sum[w(F_o^2 - F_c^2)^2/\sum(w(F_o^2)^2)]^{1/2}$; $w = 1/[s^2(F_o^2) + (xP)^2 + yP]$, $P = (F_o^2 + 2F_c^2)/3$, where $x = 0.0549$ and $y = 92.9739$.

analysis. Data were collected on a Siemens SMART CCD diffractometer with graphite-monochromated Mo K α radiation ($\lambda = 0.71073$ Å) at 293 K. All absorption corrections were performed with the SADABS program.¹³ The structure was solved by direct methods and refined by full-matrix least-squares methods on *F*² using the SHELXTL97 program package.¹⁴ A total of 14 633 reflections ($2.16 \leq \theta \leq 25.70^\circ$) were collected with 9956 unique ones (*R*_{int} = 0.0347), of which 8387 reflections with *I* > 2 σ (*I*) were used for structural elucidation. At convergence, *R*₁ (*wR*₂) was 0.0471 (0.1122) and the goodness-of-fit was 1.070. The final Fourier map had a minimum and maximum of -3.365 and 3.754 e⁻Å⁻³. All the non-hydrogen atoms were refined anisotropically. The H atoms of organic ligands were geometrically placed and refined using a riding model. However, the H atoms of water molecules have not been included in the final refinement. Experimental details for the structural determinations of **1** are presented in Table 1. Ranges of selected bond lengths and angles for **1** are listed in Table 2. Crystal data are deposited with the CCDC as No. 626918.

Results and Discussion

X-ray analysis reveals that **1** consists of two isolated [Cu(enMe)₂]²⁺ cations and one polyoxoanion {[Cu(enMe)₂(H₂O)₂][Cu₆(enMe)₂(*B*- α -SiW₉O₃₄)₂]}⁴⁻ (**1a**) encapsulating an unprecedented Cu₆ cluster aggregation (Figure 1a). **1a** is constructed from two mono-TM-supported {[Cu(enMe)₂(H₂O)][*B*- α -SiW₉O₃₄]}⁸⁻ (**1b**) moieties linked by a Cu₆ cluster, resulting in a rare bi-TM-supported sandwich structure with idealized *C*_i symmetry.

In the central Cu₆ cluster of **1a** (Figure 1b,c), six Cu²⁺ ions can be divided into two groups according to the positions at which they are located. The first group includes internal Cu2, Cu2A, Cu3, and Cu3A ions, which are just located at

Table 2. Selected Bond Lengths (Å) and Bond Angles (deg) for **1**^a

bond	dist	bond	dist
Cu(1)–O(7A)	1.990(10)	W(4)–O(8)	1.906(11)
Cu(1)–O(1A)	1.995(10)	W(4)–O(30)	1.970(10)
Cu(1)–O(5)	2.365(10)	W(4)–O(32)	2.377(10)
Cu(1)–N(2)	1.991(15)	W(5)–O(23)	1.724(10)
Cu(1)–N(1)	1.995(14)	W(5)–O(2)	1.778(10)
Cu(2)–O(4)	1.939(10)	W(5)–O(25)	1.884(10)
Cu(2)–O(7A)	1.942(9)	W(5)–O(12)	2.013(10)
Cu(2)–O(3)	1.980(10)	W(5)–O(19)	2.017(10)
Cu(2)–O(3A)	2.024(9)	W(5)–O(32)	2.341(10)
Cu(2)–O(6A)	2.303(10)	W(6)–O(22)	1.715(11)
Cu(2)–O(5)	2.489(11)	W(6)–O(13)	1.894(10)
Cu(3)–O(6A)	1.932(10)	W(6)–O(30)	1.904(10)
Cu(3)–O(2)	1.943(9)	W(6)–O(12)	1.904(11)
Cu(3)–O(1)	1.950(10)	W(6)–O(18)	1.918(9)
Cu(3)–O(5A)	1.984(10)	W(6)–O(32)	2.400(9)
Cu(3)–O(3)	2.324(10)	W(7)–O(11)	1.717(10)
W(1)–O(26)	1.713(10)	W(7)–O(4)	1.773(10)
W(1)–O(17)	1.869(10)	W(7)–O(25)	1.950(11)
W(1)–O(24)	1.892(11)	W(7)–O(29)	1.952(10)
W(1)–O(18)	1.917(9)	W(7)–O(16)	2.022(10)
W(1)–O(31)	1.930(11)	W(7)–O(21)	2.300(9)
W(1)–O(9)	2.401(10)	W(8)–O(33)	1.722(11)
W(2)–O(28)	1.719(11)	W(8)–O(5)	1.835(10)
W(2)–O(7)	1.875(10)	W(8)–O(14)	1.911(10)
W(2)–O(8)	1.935(10)	W(8)–O(29)	1.928(10)
W(2)–O(27)	1.938(12)	W(8)–O(10)	2.001(11)
W(2)–O(31)	1.945(10)	W(8)–O(21)	2.422(10)
W(2)–O(9)	2.299(9)	W(9)–O(20)	1.729(10)
W(3)–O(15)	1.722(11)	W(9)–O(10)	1.876(10)
W(3)–O(6)	1.814(10)	W(9)–O(16)	1.879(10)
W(3)–O(14)	1.921(10)	W(9)–O(13)	1.920(10)
W(3)–O(27)	1.951(11)	W(9)–O(24)	1.958(10)
W(3)–O(17)	2.002(9)	W(9)–O(21)	2.407(9)
W(3)–O(9)	2.389(9)	Si(1)–O(9)	1.637(9)
W(4)–O(34)	1.738(10)	Si(1)–O(21)	1.637(9)
W(4)–O(1)	1.869(10)	Si(1)–O(3)	1.645(10)
W(4)–O(19)	1.887(11)	Si(1)–O(32)	1.654(10)

angle	measure	angle	measure
O(7A)–Cu(1)–N(2)	168.5(7)	O(3)–Cu(2)–O(6A)	87.3(4)
O(7A)–Cu(1)–O(1A)	90.2(4)	O(3A)–Cu(2)–O(6A)	88.0(4)
N(2)–Cu(1)–O(1A)	91.9(5)	O(4)–Cu(2)–O(5)	89.5(4)
O(7A)–Cu(1)–N(1)	91.9(5)	O(7A)–Cu(2)–O(5)	84.7(4)
N(2)–Cu(1)–N(1)	84.5(6)	O(3)–Cu(2)–O(5)	88.4(4)
O(1A)–Cu(1)–N(1)	171.3(5)	O(3A)–Cu(2)–O(5)	87.1(4)
O(7A)–Cu(1)–O(5)	87.1(4)	O(6A)–Cu(2)–O(5)	173.8(3)
N(2)–Cu(1)–O(5)	104.4(6)	O(6A)–Cu(3)–O(2)	90.1(4)
O(1A)–Cu(1)–O(5)	75.2(4)	O(6A)–Cu(3)–O(1)	174.5(4)
N(1)–Cu(1)–O(5)	113.3(5)	O(2)–Cu(3)–O(1)	95.4(4)
O(4)–Cu(2)–O(7A)	90.6(4)	O(6A)–Cu(3)–O(5A)	88.9(4)
O(4)–Cu(2)–O(3)	94.1(4)	O(2)–Cu(3)–O(5A)	175.8(4)
O(7A)–Cu(2)–O(3)	171.6(4)	O(1)–Cu(3)–O(5A)	85.8(4)
O(4)–Cu(2)–O(3A)	175.7(4)	O(6A)–Cu(3)–O(3)	87.9(4)
O(7A)–Cu(2)–O(3A)	91.7(4)	O(2)–Cu(3)–O(3)	91.3(4)
O(3)–Cu(2)–O(3A)	83.3(4)	O(1)–Cu(3)–O(3)	91.2(4)
O(4)–Cu(2)–O(6A)	95.2(4)	O(5A)–Cu(3)–O(3)	92.8(4)
O(7A)–Cu(2)–O(6A)	99.2(4)		

^a Symmetry transformations used to generate equivalent atoms: (A) $-x + 1, -y + 1, -z + 1$.

the four vacant sites of two **1b** moieties to form a sandwich [Cu₄(SiW₉O₃₄)₂]¹²⁻ fragment. Interestingly, the independent Cu2 and Cu3 ions exhibit different configurations. Cu2 is bonded to six O atoms from two **1b** moieties to form a distorted octahedron with the O5 and O6 atoms occupying the axial positions, while Cu3 only defined by five O atoms from two **1b** moieties, forming a distorted square pyramid with the O3 atom occupying the axial position. Thus, two CuO₆ octahedra and two CuO₅ square pyramids are linked

(13) Sheldrick, G. M. *SADABS, Program for Siemens Area Detector Absorption Corrections*; University of Göttingen: Göttingen, Germany, 1997.

(14) (a) Sheldrick, G. M. *SHELXS97, Program for Crystal Structure Solution*; University of Göttingen: Göttingen, Germany, 1997. (b) Sheldrick, G. M. *SHELXL97, Program for Crystal Structure Refinement*; University of Göttingen: Göttingen, Germany, 1997.

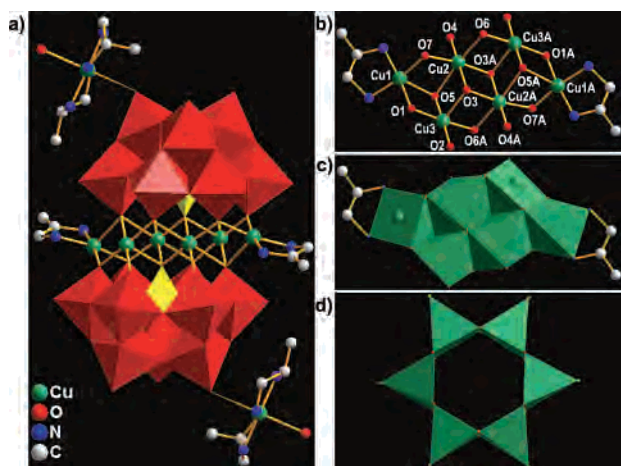


Figure 1. (a) Structure of polyoxoanion **1a**. Color codes: WO_6 , red; SiO_4 , yellow. (b, c) Ball-and-stick and polyhedral representations of the Cu_6 hybrid unit in **1**, respectively. (d) Polyhedral representation of the Cu_6 unit in ref 9.

together by sharing edges to form an unexpected defective rhombic Cu_4 unit, differing from the usual rhombic M_4 units with four edge-sharing MO_6 octahedra in lots of reported sandwich TMSPs.³ The second group includes external Cu1 and Cu1A ions. The independent Cu1 ions is defined by three O atoms from two **1b** moieties and two N atoms of one enMe ligand, forming a distorted square pyramidal configuration with the O5 atom occupying the axial position. The two external square pyramids ($\text{Cu}(1)\text{O}_3\text{N}_2$ and $\text{Cu}(1\text{A})\text{O}_3\text{N}_2$) are further attached to the internal Cu_4 unit by edge-shared to form a unique nearly coplanar and beltlike Cu_6 cluster aggregation. Searches of the Cambridge Crystallographic (<http://www.ccdc.cam.ac.uk>) and Inorganic Crystal (<http://icsdweb.fiz-karlsruhe.de>) Structure Databases show no such Cu_6 cluster has been reported. Therefore, the structural details of this central Cu_6O_{14} fragment are of interest. Both the octahedral and square pyramidal coordination spheres of Cu^{2+} centers are Jahn–Teller distorted. The equatorial Cu–O distances range from 1.932(10) to 2.025(9) Å, whereas the axial Cu–O distances range 2.304(10)–2.490(11) Å. The crystallographic independent Cu–O–Cu angles of the central Cu_6O_{14} fragment are 106.9(1)° (O1), 93.18(1)° (O6), and 105.8(1)° (O7), respectively. The angles around O3 and O5 range 91.34(1)–96.74(1) and 81.06(1)–92.17(1)°, respectively. The independent $\text{Cu}\cdots\text{Cu}$ separations are as follows: $\text{Cu}1\cdots\text{Cu}2$, 3.16 Å; $\text{Cu}1\cdots\text{Cu}3$, 3.15 Å; $\text{Cu}2\cdots\text{Cu}3$, 3.13 Å; $\text{Cu}2\cdots\text{Cu}2\text{A}$, 2.99 Å; $\text{Cu}3\cdots\text{Cu}2\text{A}$, 3.09 Å.

Crystal packing of **1** can be seen in Figure 2; the anions **1a** are stacked along both *a*- and *b*-axis directions, forming a POM layer that is parallel to the *ab*-plane. These POM layers are further stacked in parallel in AAA sequence along the *c*-axis to form three-dimensional stacking structure with supporting $[\text{Cu}(\text{enMe})_2(\text{H}_2\text{O})]^{2+}$ and isolated $[\text{Cu}(\text{enMe})_2]^{2+}$ cations residing in the space between the POM layers. Although the $[\text{A}-\alpha\text{-SiW}_9\text{O}_{34}]^{9-}$ ions were used as starting material, the products contain $[\text{B}-\alpha\text{-XW}_9\text{O}_{34}]^{9-}$ units, indicating that the isomerization of $[\text{A}-\alpha\text{-SiW}_9\text{O}_{34}]^{10-} \rightarrow [\text{B}-\alpha\text{-SiW}_9\text{O}_{34}]^{10-}$ must have taken place during the course of the reaction. Similar isomerization of $[\text{A}-\alpha\text{-PW}_9\text{O}_{34}]^{9-} \rightarrow [\text{B}-\alpha\text{-$

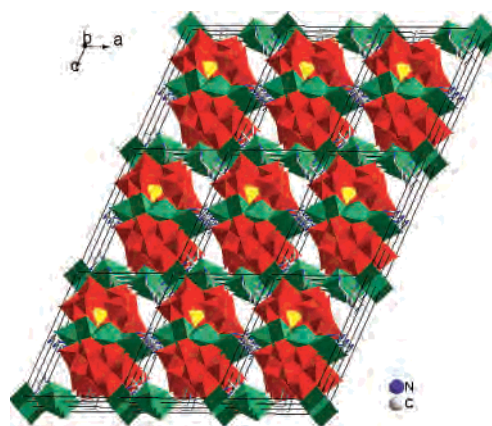


Figure 2. View of crystal packing of **1** along the *b*-axis. All the isolated water molecules and hydrogen atoms are omitted for clarity. Color codes: WO_6 , red; SiO_4 , yellow.

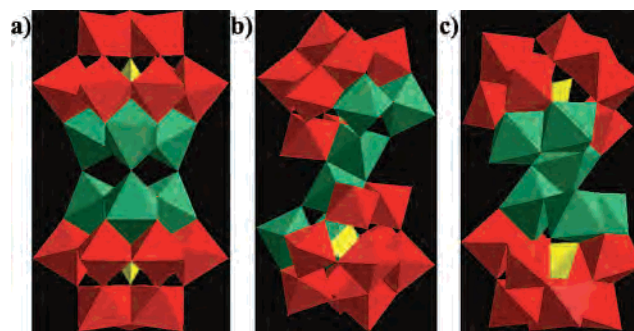


Figure 3. Polyhedral representations of (a) $\text{Fe}_6\text{Ge}_2\text{W}_{18}$ or $\text{Fe}_6\text{Si}_2\text{W}_{18}\text{-1}$; (b) $\text{Fe}_6\text{Si}_2\text{W}_{18}\text{-2}$; (c) $\text{Ni}_6\text{Si}_2\text{W}_{18}$. Color codes: WO_6 , red; FeO_6 or NiO_6 , green; GeO_4 or SiO_4 , yellow.

$\text{PW}_9\text{O}_{34}]^{9-}$ has been demonstrated in the solution upon heating in several reports in the literature.^{30,15}

Compared with the first Cu_6 -containing polyoxoanion $[(\text{CuCl})_6(\text{AsW}_9\text{O}_{33})_2]^{12-}$ ($\text{Cu}_6\text{As}_2\text{W}_{18}$),⁹ the remarkable differences are as follows: (1) **1a** is a polyoxoanion based on $[\text{SiW}_9\text{O}_{34}]^{10-}$ units, while $\text{Cu}_6\text{As}_2\text{W}_{18}$ is a polyanion based on $[\text{As}^{\text{III}}\text{W}_9\text{O}_{33}]^{9-}$ units in which the lone pair of electrons on the As^{III} atom does not allow the closed Keggin unit to form.^{3m,s} (2) Due to the different structural feature between $[\text{SiW}_9\text{O}_{34}]^{10-}$ and $[\text{AsW}_9\text{O}_{33}]^{9-}$, the encapsulated Cu_6 core in **1a** is a beltlike structure with edge-sharing combination of CuO_6 octahedra, CuO_5 , and CuO_3N_2 square pyramids, while the Cu_6 core in $\text{Cu}_6\text{As}_2\text{W}_{18}$ is a hexagon structure made of six edge-shared CuO_4Cl square pyramids (Figure 1d). (3) The Cu_6 core in **1a** is an inorganic–organic hybrid cluster, while the Cu_6 core in $\text{Cu}_6\text{As}_2\text{W}_{18}$ is an inorganic cluster. Additionally, the configuration of Cu_6 core in **1a** is also remarkable different from the other M_6 cores in several reported M_6 -substituted polyoxotungstates, such as $[\text{Fe}_6(\text{OH})_3(\text{A}-\alpha\text{-GeW}_9\text{O}_{34}(\text{OH})_3)_2]^{11-}$ ($\text{Fe}_6\text{Ge}_2\text{W}_{18}$),⁶ $[\{\text{Ni}_6(\text{H}_2\text{O})_4(\mu_2\text{-H}_2\text{O})_4(\mu_3\text{-OH})_2\}(\chi\text{-SiW}_9\text{O}_{34})_2]^{10-}$ ($\text{Ni}_6\text{Si}_2\text{W}_{18}$),⁷ $[(\alpha\text{-SiFe}_3\text{W}_9(\text{OH})_3\text{O}_{34})_2(\text{OH})_3]^{11-}$ ($\text{Fe}_6\text{Si}_2\text{W}_{18}\text{-1}$), and $[(\alpha\text{-Si}(\text{FeOH})_2)_2\text{FeW}_9(\text{OH})_3\text{O}_{34}]^{8-}$ ($\text{Fe}_6\text{Si}_2\text{W}_{18}\text{-2}$).¹⁰ As shown in Figure 3a, the central Fe_6 core in $\text{Fe}_6\text{Ge}_2\text{W}_{18}$ or $\text{Fe}_6\text{Si}_2\text{W}_{18}\text{-1}$ exhibits a trigonal-prismatic fragment composed of six

(15) Knoth, W. H.; Domaille, P. J.; Harlow, R. L. *Inorg. Chem.* **1986**, *25*, 1577.

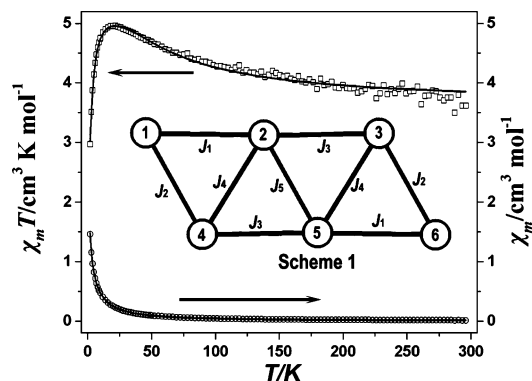


Figure 4. Temperature dependence of χ_m (○) and $\chi_m T$ (□) values for **1**. The solid lines correspond to the best-fit curves using the parameters described in the text.

corner-sharing FeO_6 octahedra, while the central Fe_6 core in **Fe₆Si₂W₁₈-2** is build up of two equivalent Fe_3O_{15} trimers linked together by a single edge (Figure 3b). In the **Ni₆Si₂W₁₈**, six central NiO_6 octahedra are joined together by edge- or corner-sharing to form a “Z” type Ni_6 unit (Figure 3c). In comparison with the above-reported M_6 cores, **1a** represents a new type of inorganic–organic hybrid M_6 -substituted sandwich polyoxotungstate.

The TG curve of **1** shows the first weight loss of 2.04% in the temperature range 52–113 °C, corresponding to the loss of six H_2O molecules (calcd 1.82%)/formula unit. The second weight loss of 13.08%, which occurs in multiple steps from 210 to 609 °C, is attributed to the loss of 10 enMe molecules (calcd 12.48%). Assuming that the residue corresponds to SiO_2 , WO_3 , and CuO , the observed weight loss (15.12%) is in good agreement with the calculated value (14.29%).

Since **1** contains a well-isolated central Cu_6 unit with an unusual geometry, it is of interest to investigate its magnetic properties. The magnetic susceptibility of **1** was measured at 2–300 K (Figure 4). The experimental $\chi_m T$ value at room temperature is $3.61 \text{ cm}^3 \cdot \text{mol}^{-1} \cdot \text{K}/\text{formula}$, which is expected for 10 magnetically uncoupled Cu^{2+} ion ($3.75 \text{ cm}^3 \cdot \text{mol}^{-1} \cdot \text{K}$, assuming $g = 2$). Upon cooling, the $\chi_m T$ values increase to a maximum of $4.95 \text{ cm}^3 \cdot \text{mol}^{-1} \cdot \text{K}$ at 22 K and then decrease to $2.96 \text{ cm}^3 \cdot \text{mol}^{-1} \cdot \text{K}$ at $T = 2 \text{ K}$, where the sudden decrease might be attributed to intermolecular interactions within the compound. The behavior suggests that there exist overall ferromagnetic interactions. The temperature dependence of the reciprocal susceptibilities ($1/\chi_m$) obeys the Curie–Weiss law above 75 K with $\Theta = 17.85$ (Figure 5), which support the presence of overall ferromagnetic coupling between the Cu^{2+} ions.

Considering the C_i symmetry of the Cu_6 unit in **1**, the magnetic data can be simulated in terms of the five exchange constants J_1 – J_5 as shown in Scheme 1 (inset of Figure 4), where the numbers 1–6 correspond to the Cu1, Cu2, Cu3A, Cu3, Cu2A, and Cu1A of Figure 1b, respectively. Since diagonal interactions between Cu^{2+} ions (Cu1...Cu5, Cu2...Cu6, and Cu3...Cu4) with significantly long distance (more than 5.3 Å) within the Cu_6 unit are weak enough to be assumed to be negligible. Following the numbering

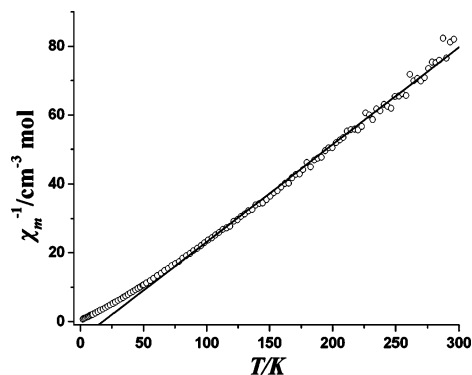


Figure 5. Temperature dependence of χ_m^{-1} (○) for **1**. The solid line is best fit according to the Curie–Weiss law.

scheme, the magnetic data of **1** are simulated on the basis of the spin Hamiltonian in eq 1 using the package MAGPACK.¹⁶ The contribution of the mononuclear Cu^{2+} species in **1** is incorporated through Curie law.

$$\hat{H} = -2J_1(\hat{S}_1\hat{S}_2 + \hat{S}_5\hat{S}_6) - 2J_2(\hat{S}_1\hat{S}_4 + \hat{S}_3\hat{S}_6) - 2J_3(\hat{S}_2\hat{S}_3 + \hat{S}_4\hat{S}_5) - 2J_4(\hat{S}_2\hat{S}_4 + \hat{S}_3\hat{S}_5) - 2J_5\hat{S}_2\hat{S}_5 \quad (1)$$

Additionally, a parameter zJ accounts for the intermolecular interactions for **1** by using molecular field approximation ($\chi_{\text{mol}} = \chi_{\text{M}}/[1 - \chi_{\text{M}}(2zJ/N_{\text{A}}g^2\mu_{\text{B}}^2)]$). The best-fit parameters obtained are $J_1 = 12.70 \text{ cm}^{-1}$, $J_2 = -2.56 \text{ cm}^{-1}$, $J_3 = 30.96 \text{ cm}^{-1}$, $J_4 = 30.97 \text{ cm}^{-1}$, $J_5 = 39.40 \text{ cm}^{-1}$, $zJ = -0.48 \text{ cm}^{-1}$, $g = 1.97$, and $R = 3.15 \times 10^{-4}$ (the error factor R is defined as $\sum[(\chi_{\text{M}}T)_{\text{obs}} - (\chi_{\text{M}}T)_{\text{calc}}]^2/\sum[(\chi_{\text{M}}T)_{\text{obs}}^2]$). These results show that the magnetic properties of the unique Cu_6 unit are a combination of both ferromagnetic and antiferromagnetic exchange interactions. Since the small and negative parameters of J_2 and zJ show that the Cu1...Cu4 interaction and intermolecular interaction are weak antiferromagnetic, the overall interactions in Cu_6 unit are ferromagnetic. For di- μ -hydroxo-bridged copper dimers, a classical correlation between the Cu–O–Cu bond angle (Φ) and the experimental exchange constant (J) ($J = -74.53\Phi + 7270 \text{ cm}^{-1}$) indicates that those complexes are antiferromagnetic for $\Phi > 98^\circ$ but ferromagnetic for smaller angles.¹⁷ The calculations based on the above correlation and the observed Cu–O–Cu angle in **1** also can predict that the exchange parameters J_1 – J_5 should be positive and parameter J_2 should be negative.

Conclusions

In summary, a novel Cu_6 -containing TMSPs **1** has been synthesized, which contains the largest number of paramagnetic TMs of all sandwich silicotungstates known. In addition, the central Cu_6 unit exhibits a unique geometry. The successful synthesis of **1** shows that hydrothermal techniques offer an effective way for making high-nuclear TMSPs based on lacunary anions. Further work is in progress

- (16) (a) Borrás-Almenar, J. J.; Clemente-Juan, J. M.; Coronado, E.; Tsukerblat, B. S. *Inorg. Chem.* **1999**, *38*, 6081. (b) Borrás-Almenar, J. J.; Clemente-Juan, J. M.; Coronado, E.; Tsukerblat, B. S. *J. Comput. Chem.* **2001**, *22*, 985.
 (17) Crawford, V. H.; Richardson, H. W.; Wasson, J. R.; Hodgson, D. J.; Hatfield, W. E. *Inorg. Chem.* **1976**, *15*, 2107.

for making other new TMSPs made of high-nuclear metal cluster aggregations and other types of lacunary precursors (e.g., $[XW_{10}O_{36}]^{n-}$ and $[X_2W_{15}O_{56}]^{n-}$) or mixed multilacunary precursors under hydrothermal conditions.

Acknowledgment. This work was supported by the 973 Program (No. 2006CB932900), the NSF of China (Nos. 20473093/20271050), the NSF of Fujian Province (Nos.

E0510030/2005HZ01-1), and the Key Project from CAS (No. KJCX-YW-H01).

Supporting Information Available: Crystal data in CIF format, an IR spectrum, and a TG plot. This material is available free of charge via the Internet at <http://pubs.acs.org>.

IC070160C